LIP-STUDENTS-23-7

Energy calibration and simulation for the SNO+ experiment

André Rodrigues[1,a]

[1] *NOVA School of Science and Technology, Caparica, Portugal*

Project supervisor: Valentina Lozza

October 11, 2023

Abstract. Calibrations are an important part in any experiment. This paper summarizes the work done in the calibrations for SNO+ "Scintillator phase" during my internship. The calibration was based on a coincidence analysis of an Am-Be source.The source was selected because it emits a neutron and a gamma in coincidence, which allows a clear identification. Data from two separated calibration campaigns have been used. Results have been compared against each other and Monte Carlo simulations. A discrepancy between data and simulation s has been found, with latter underestimating the energy of both neutrons and gammas. Furthermore, a very different spacial distribution of the events at the edges of acrylic has been identified when the data are compared to Monte Carlo, affecting the temporal distribution of those events. Mismodeling of the optical properties of acrylic, creating a different distribution of the detected events has been identified as a probable cause. Finally, a double 2.2Mev + 2.2MeV γ's coincidence was studied and connected with the $^{9}_{4}$Be(n,2n) reaction in the source.

Keywords: SNO+, Energy calibration, Am-Be calibration source, Analysis of coincidence

1 Introduction

1.1 The SNO+ detector

SNO+ is the follow-up of the SNO experiment (Sudbury Neutrino Observatory), detector built in a mine in Sudbury, Canada, with the objective of studying neutrino properties and interactions. The active medium is a liquid scintillator which emits light when interacting with charged particles, allowing the observation and study of neutrinos by their interactions with electrons and/or protons of the medium.

Even with the main focus of studying the neutrinoless double beta decay, due to the high purity materials, and strategic location 2km underground in a old nickel mine in Sudbury, which filters the majority of the cosmic rays, SNO+ can study other physics topics like solar neutrinos, geo and reactor anti-neutrinos, supernovae neutrinos and anti-neutrinos and some other rare decays.

The SNO+ detector is a 6m radius and a 5cm thickness acrylic vessel (AV), filled with about 780 tonnes of scintillator, Linear Alkyl Benzine (LAB), chosen by its optical properties and chemical compatibility with the acrylic. This acrylic vessel is then surrounded by about 9500 Hamamatsu R1408 photomultipliers (PMT's) facing inwards for 54% coverage. The vessel and the PMT's are then submerged in 7000 tonnes of ultra-pure water filling the cavity excavated in the Rock (see Figure 1).

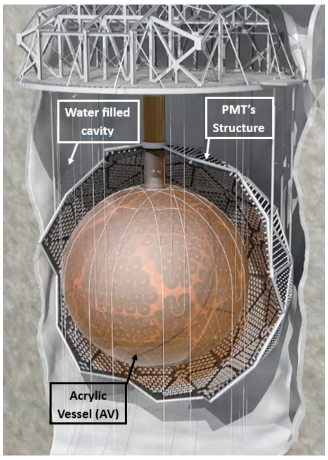

Figure 1. View of SNO+ structure model

1.2 The Scintillator phase

The SNO+ experimental phase started with the "water-phase" (2017), when the detector was full of ultra-pure water serving as a Cherenkov detector, being able to obtain the first evidences that reactor anti-neutrinos can be detected and studied by this type of detector, information that will be important in later phases[2].

The second phase, or "Scintillator phase", in which the acrylic vessel is filled with LAB scintillator is focused on the study of solar,geo and reactor anti-neutrinos, and the phase in which this work is centered. In this phase the detector was calibrated using an Am-Be source that will better explained in subsection 1.3.

In this phase the acrylic vessel is filled with about 780 tonnes of LAB with 2.2g/L of 2,5-diphenyloxazole (PPO). The combination of this 2 materials shifts the emitted lights wavelength to the region where the PMT's have the greatest sensitivity, increasing the efficiency of the detector.

The filling of the detector started in July 2019 and consisted in slowly replacing the high purity water with the scintillator. Due to the COVID-19 pandemic, the replace-

[a]e-mail: andre.f.rodrigues00@gmail.com

ment stopped in March 2020 until October 2020, making SNO+ to take data in the so called "Partial fill Period", where there were 365 tonnes of scintillator on top of the high-purity water inside the AV. The scintillator filling ended in March 2021 starting the PPO filling campaign ending in May 2022, from which SNO+ started to continuously take data that is now being used for the scintillator phase data analysis. Such data, more specifically the May 2022 and August 2022 calibration data, will be the working material of this internship.

The last phase called "Tellurium loaded scintillator phase" will finally study the neutrinoless double beta decay of tellurium 130, a theoretical process with purely electron emission during a beta decay, process that has not been observed to the date of this work.

1.3 Am-Be calibration source

The used Am-Be source was produced in 2005 at SNOLAB and since then it has been stored in the SNOLAB storage. The fully encapsulated source is a 6cm diameter and 8 cm height cylinder with a rate of (67.4±0.7) neutrons per second measured at the time of deployment (2018) when it was placed just outside the acrylic vessel (see Figure 2).

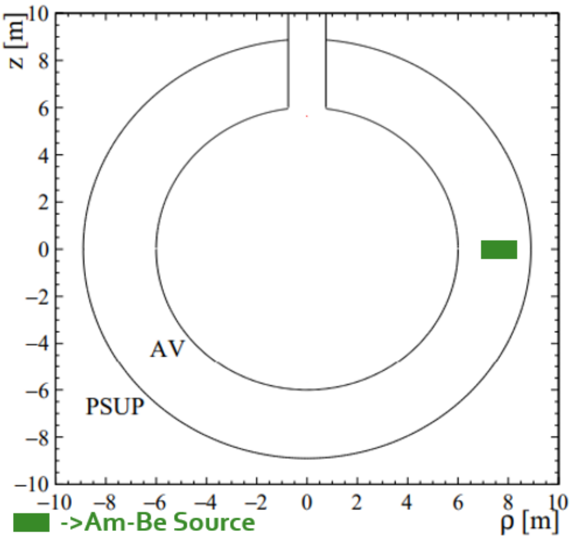

Figure 2. SNO+ schematic showing where the Am-Be source was positioned during this calibration data collection, at the 6m radius we have the acrylic vessel (AV) and at 9m we have the PMT's support structure (PSUP).

The Am-Be calibration source consists of a compound of 241-Americium nuclei, which undergo α-decay with a half-life close to 432.2 years, and a ^{9}Be target that will absorb the α's and, among other things produce a ^{13}C nucleus that immediately decay to ^{12}C nucleus and a neutron, the ^{12}C can be in an excited state (60% of the times) and immediately de-excite emitting a 4,4MeV γ serving as the prompt event. The majority of the neutrons formed in this reaction will rapidly thermalize and get captured by Hydrogen nuclei producing ^{2}H nuclei (deuterium) and emitting a 2.2MeV γ serving as the main delay event. Other excited states from ^{12}C and other reaction happening in the Am-Be source, for example other events that produce neutrons, will also contribute in small amounts to the events detected. We can use this extra events as calibrations tools as well.

The analysis of the Am-Be data is based on the coincidence thecnique by using the 4.4MeV γ as the prompt event and the neutron capture 2.2MeV γ as the delay event. This makes sure the neutrons under study are from Am-Be source and not from ambient noise.

2 Energy calibration

2.1 Energetic events sources/reactions

As explained in 1.3. ,there's more than one reaction or chain reactions emitted by the source at any time, understanding these reactions and what energies have the gamma rays emitted is a crucial step towards understanding the energy spectrum measured by the detector.

The starting reaction is the alpha decay plus a gamma ray emission: 241-Americium decays with an averaging 5.477MeV alpha energy.

$^{241}_{95}\mathrm{Am} \xrightarrow{432.2\,\mathrm{y}} {}^{237}_{93}\mathrm{Np} + {}^{4}_{2}\alpha + 59{,}5409\,\mathrm{keV}$

From here we start having a mix of possible reactions being the most common the α-particle captured by a ^{9}Be nuclei creating an unstable ^{13}C nuclei.

$^{9}_{4}\mathrm{Be} + {}^{4}_{2}\alpha \longrightarrow {}^{13}_{6}\mathrm{C}^{*}$

^{13}C will, with a half-life of 61fs[5], decay to a more stable ^{12}C through various paths being, the most common, the one with about 60% of the decays[7].

$^{13}_{6}\mathrm{C}^{*} \xrightarrow{61\,\mathrm{fs}} {}^{12}_{6}\mathrm{C}^{*} + {}^{1}_{0}\mathrm{n} + 1.27\,\mathrm{MeV}$
$^{12}_{6}\mathrm{C}^{*} \longrightarrow {}^{12}_{6}\mathrm{C} + (4.43\,\mathrm{MeV})\gamma$

Followed by:

$^{1}_{1}\mathrm{H} + {}^{1}_{0}\mathrm{n} \longrightarrow {}^{2}_{1}\mathrm{H} + (2.2\,\mathrm{MeV})\gamma$

This reaction is the reason why this source was among the chosen to calibrate the scintillator phase, due to the coincidence 2.2MeV from the neutron capture and 4.4MeV gammas from the decay of ^{12}C* to a stable state[2].

Even if this decay chain is, with an average capture time of 200μs, the most probable, other less common decays can be identified for $^{13}_{6}$C coming from $^{241}_{95}$Am. Such as the de-excitation directly to the ground state of $^{13}_{6}$C (40%) with no γ [5],[7]:

$^{13}_{6}\mathrm{C}^{*} \longrightarrow {}^{12}_{6}\mathrm{C} + {}^{1}_{0}\mathrm{n} + 5.7\,\mathrm{MeV}$

Followed by:

$^{1}_{1}\mathrm{H} + {}^{1}_{0}\mathrm{n} \longrightarrow {}^{2}_{1}\mathrm{H} + (2.2\,\mathrm{MeV})\gamma$

Due to the fact that all these reactions release a 2.2MeV gamma from the neutron capture, the coincidence analysis allows a separation among them since the prompt events are different from one another.

Another possible reaction is the $^{9}_{4}$Be(n,2n) [3],[6] where the bombardment of the beryllium nuclei by neutrons have a non zero chance to emit 2 or more neutrons.

$^{9}_{4}\mathrm{Be} + {}^{1}_{0}\mathrm{n} \longrightarrow 2\,{}^{4}_{2}\alpha + 2\,{}^{1}_{0}\mathrm{n} - 1.57\,\mathrm{MeV}$

Or:

$^{9}_{4}\mathrm{Be}^{*} \longrightarrow {}^{8}_{4}\mathrm{Be} + {}^{1}_{0}\mathrm{n} - 1.65\,\mathrm{MeV}$

Or:

$^{9}_{4}\text{Be}^{*} \longrightarrow 2\,^{4}_{2}\alpha + ^{1}_{0}\text{n} - 1.564\,\text{MeV}$

Always followed by:

$^{1}_{1}\text{H} + ^{1}_{0}\text{n} \longrightarrow ^{2}_{1}\text{H} + (2.2\,\text{MeV})\gamma$

Knowing all the reactions happening at any time and having a good understanding of the energy such reactions release is very important to identify the peaks in the energy spectrum, to then later compare against the measured calibration source energy spectrum.

Special importance is given to the $^{9}_{4}$Be(n,2n) reaction due to the fact that this reaction emits 2 instead of 1 neutrons.

2.2 Analysis of coincidences

The calibration analysis using the Am-Be source works by using the difference in time between 2 consecutive (prompt and delay) events above a certain threshold in the number of PMT's hits. This events are then filtered by lower and upper bounds in energy or PMT's hits that are selected to include the majority of the signal needed for the experiment in question.

The threshold used for the number of PMT's hits for the data analysis was 200 (ca. 0.7MeV) due to the fact that below this level we expect mainly background events, not useful for the wanted analysis.

In my analysis a time difference between prompt and delay event of 4000μs was used, this value was chosen having in consideration that the half-life of the neutron-proton capture calculated in the "water phase" measurements[2] was 143μs, making sure that most of the wanted events will get captured in this time of 28 half-life.

2.3 Energy calibration

As said in the introduction, this work uses the SNO+ calibration data from May of 2022, just after the Scintillator filling, and August 2022. Both data set were taken approximately in the same conditions and should have the same events distributions and energy spectrum. However, to make sure the experiment really has no variability over time, comparing these 2 data sets is of great importance.

When comparing the data from this 2 time periods 2 main differences were found illustrated in figure 3 and 4, where we can see, that the energy of the 4.4MeV prompt events has closely the same distribution in both periods but has the mean value shifted by (0.075±0.004)MeV. The same effect is seen in the 2.2MeV delay events where we have a similar distribution but a similar shift of (0.034±0.008)MeV. The difference is +1.7% in the 4.4MeV prompt events and +1.5% increase in the 2.2MeV delay events, meaning the shift in energy increases as energy level increases. The observed shifts might be caused by the non-homogeneity of the wavelength shifting material (PPO) in May due to the close temporal proximity to the PPO addition period compared to August.

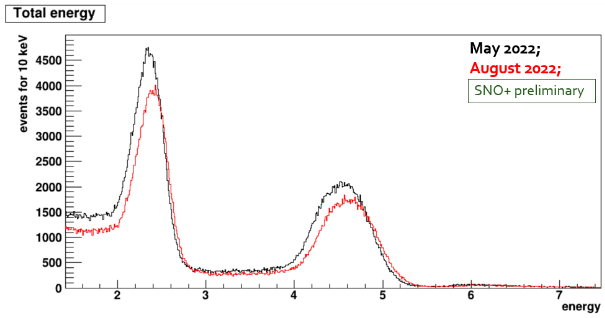

Figure 3. Energy spectrum for May and August Am-Be calibration data.

Another important comparison is the energy peak position in data compared to the expected values for such reactions where we have both the 4.43MeV[6],[7] from $^{13}_{6}$C, the 6.128MeV[10] from the ^{16}O(n,nγ)^{16}O reaction and the 2.223MeV[6],[8] from the thermal neutron capture by hydrogen nuclei.

Theoretical	May	Aug	Ratio May	Ratio Aug
6.128	6.143	6.136	1.002	1.001
4.43	4.540	4.615	1.025	1.042
2.223	2.349	2.383	1.057	1.072

Table 1. Comparison mean energy (MeV) between the reconstructed values in data and the expected values from literature [5,6,7]. Ratio to theoretical values also given.

An important observation to be made is in the 6.1MeV prompt (see Table 1), from which we can extract a much closer mean peak value to this higher energy prompt showing, again, a decrease in the overestimation of the events energies.

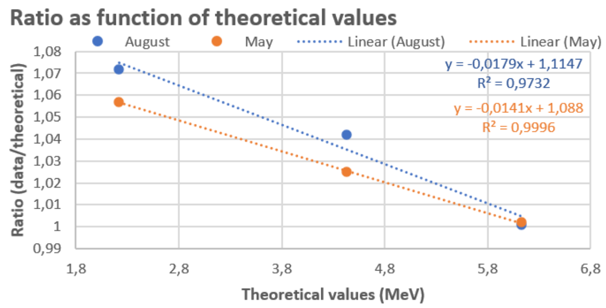

Figure 4. Plot of Ratios as function of theoretical values showing a linear dependence.

Figure 4 shows a very clear linear dependence in energies or both months when compared to the theoretical value. The difference between the 2 linear trends can, again, be caused by the non-homogeneity of the LAB+PPO mixture in May.

Due to the high volume of events in the 2.2MeV and the 4.4MeV range the statistical uncertainty is lower than 0.5%, however the 6.128MeV due to only representing a small fraction of events the statistical uncertainty is close to 1%.

2.4 Position calibration

Other noticeable difference is the mean value for the positions of the events in the Z axis, where the delay event is 1.8cm lower in August when compared to May. In the prompt event we have the same effect with a shift by 1.5cm. This shift might be due to the variation in position of the Am-Be source capsule during deployment.

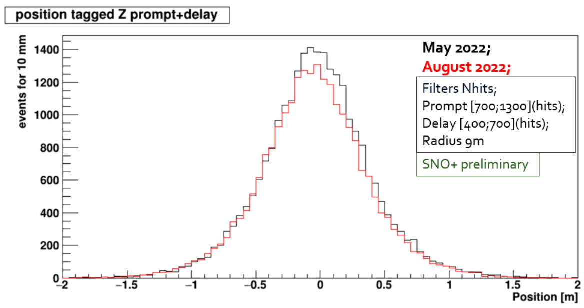

Figure 5. Position of all events in Z for May and August data. A shift between May and August is visible

2.5 Time difference from coincident events

2.5.1 Energy and Nhits time difference discrepancy

In this context the time difference is the time between the 4.4MeV prompt event from the ^{12}C de-excitation and the 2.2MeV delay event from the capture of the neutron by the hydrogen in the Scintillator.

When analysing the time difference between the events in coincidence a big problem was detected, the distribution of the events had a considerable difference depending if the events were filtered/selected by Nhits or by energy, as we can see in figure 6.

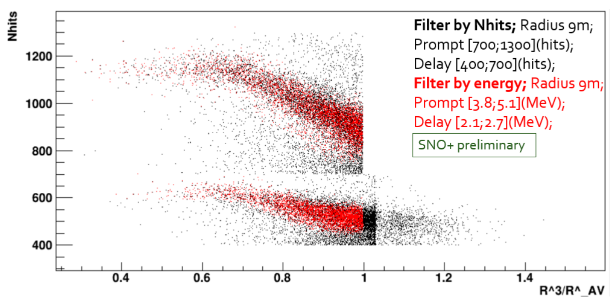

Figure 6. Nhits count in R^3/R^3_AV for the prompt (top) and delay (bottom) events in Nhits and Energy.

Figure 6 shows clearly the problem: There's a chunk of events not accounted for when the energy selector is used. The events are mainly inside the acrylic material and in the space between the vessel and the PMT's support structure. Despite a selection using energy being the best way to avoid background noise, giving a better data set to work with, this missing data creates a bias in the events selected by energy, losing important information.

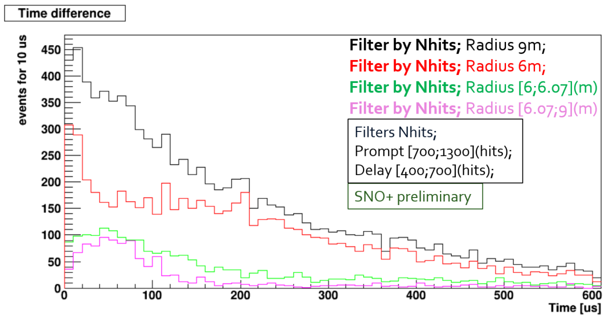

Figure 7. Time difference between the prompt and delay events in the Am-Be calibration source with different cuts in Radius.

Figure 7 shows the time difference between events for different radii, counting also with the information that had been lost as shown in Figure 6. As we can see the events in the acrylic and outside the AV have a time difference from 10 to 200 μs, this time difference coincides with the lost events when energy is used completing the expected exponential behavior of the event.

Consequently, the best way to analyse the data is by using the Nhits selector inside the 9m radius, despite the increase in background noise.

2.5.2 Full events time difference

When delay events are selected using Nhits cut in the full (9m Radius) volume, the time difference between the prompt and delay events is very similar between May and August data and can easily be fitted by a simple exponential decay plus a background constant.

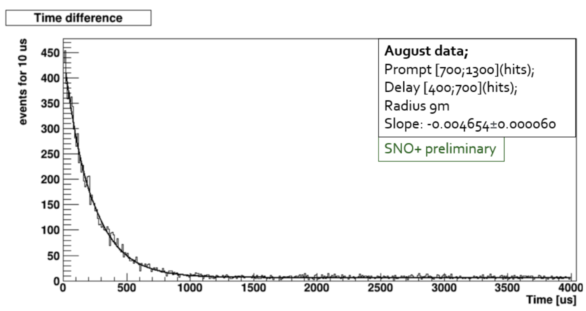

Figure 8. Time difference between the prompt and delay events in the Am-Be calibration source fitted by an exponential plus a constant (background).

Figure 8 shows the result of the fitted time difference for the Am-Be source in the conditions stated above, this fit yields a capture time constant of τ =215 $\pm$ 3 μs, agreeing with the water the error could have been smaller if the problem in 2.5.1 didn't increase the number of the background events.

Looking at Figure 7, it looks like while the faster time difference captures are happening mostly inside the ultra-pure water the slower time differences are happening in the Scintillator.

The value in the "water phase" was calculated in with the data from a source in the middle of the detector, having a more stable efficiency and only one active medium, while the source in the "Scintillator phase" is outside the vessel and the events are scattered across zones with very different efficiencies of detection which can influence the overall time constant obtained in the fit.

3 Double 2.2MeV gamma coincidence

During the work for this internship there were detected coincidences between two 2.2MeV γ events at a rate much higher of what we would be expected by random chance, close to 6600 events in August 2022 more then half of the 12400 events detected with a 4.4MeV prompt event.

In my understanding there were 2 potential explanations:

1.The possibility of being just a false coincidence, where by random chance 2 gammas of the same energy are detected in coincidence even if the original events are unrelated. This fact should contribute,in small quantities, to the amount of coincidences happening but that should not be enough to explain it. Moreover, if that was the case, the time difference graph would also be flat due to the events random coincidence (see the higher tail in Figure 9 compared to Figure 8).

2.The possibility of a different reaction, or chain of reactions, from the Am-Be calibration source, that emits 2 or more neutrons close enough in time that they are captured in coincidence. The reaction then found to explain this event is $^9_4$Be(n,2n) [3],[6], where the bombardment of the beryllium nuclei by neutrons have a non zero chance of emitting 2 or more neutrons that will then thermalize and get captured. Due to the simultaneousness of these neutrons adjusting the nhits selection for the prompt events will return events in coincidence with an exponential time difference.

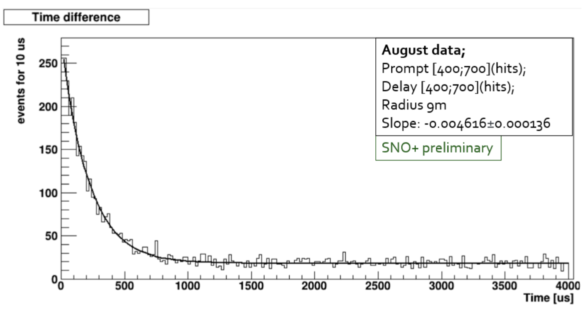

Figure 9. Am-Be calibration source time difference fitted by an exponential and an background constant for the coincidence of 2 2.2MeV gammas as prompt and delay events.

Figure 8 and 9 show the time difference graph from both the options for the signal, prompt 4.4MeV and 2.2MeV, with the normal 2.2MeV delay event. Due to the exponential behavior of the function, we can exclude the possibility of false coincidences, the graph in that case, in fact, have a larger flat tail.

This clean exponential behavior is what would be expected by the $^9Be(n,2n)$ reaction, where any neutron could be the first to get captured and still the second capture would create this exponential behavior. Another strong support to the $^9Be(n,2n)$ reaction is the fact that the exponential constant (-0.004628±0.00014) corresponding to a half-life of 150±5μs is the same as the one from the 4.4MeV prompt coincidence.

4 Monte Carlo simulations

Verifying if the data is in agreement with the known physics is very important to crosscheck the detector performance. To do so we use Monte Carlo simulations (MC), which is a mathematical model used to predict, in this case, how particles, with their probabilistic behavior, will interact and behave if placed under the same condition as in data. Verifying that the simulation reproduces correctly calibration data, is essential to trust the detector model for other, more complicated events.

4.1 Energy calibration

The same comparisons done for the data acquired in different months will be done for the MC simulations of SNO+, this comparisons is important to build a better simulation of the experiment.

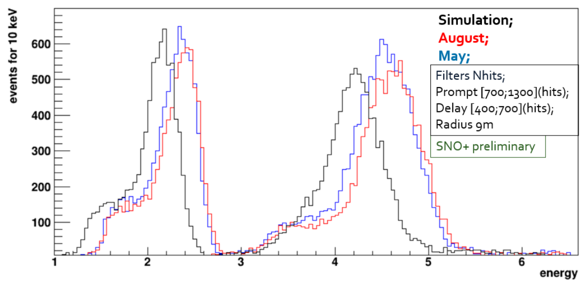

Figure 10. Reconstructed energies in the simulation compared to the ones in the data.

Figure 10 makes easy to identify the discrepancy between the data and the simulations, reaching over 10% in some situations.

Simulation	May	Aug	Ratio May	Ratio Aug
5.717	6.143	6.136	1.075	1.073
4.202	4.540	4.615	1.080	1.098
2.146	2.349	2.383	1.095	1.110

Table 2. Comparison between the mean peak energies (MeV) and the ratios (data/sim).

Theory	Simulation	Ratio Simulation
6.128	5.717	0.931
4.43	4.202	0.949
2.223	2.146	0.965

Table 3. Comparison between the mean peak energies (MeV) and its ratio

Table 2 and 3 compares all mean peak energies from which we can find that MC simulations are underestimating the energies of the 2 main processes, while SNO+ data is overestimating them in both cases. It is highly probable that the main problem is a not fully corrected simulation. A possible explanation is the modeling of the LAB+PPO medium properties creating these shifts in the mean energies at large radii.

The third value, 6.128MeV, coming from one other possible reaction happening in SNO+ (^{16}O(n, nγ)^{16}O)[10], shows a different behavior in the data, having an higher energy mean peak in May instead that August and a more stable behavior between the months. Simulation, instead, shows a consistent trend, with a larger discrepancies for higher energies.

It is advised to increase statistics of this energy point to reduce the uncertainty at high (>5MeV) energies.

4.2 Position calibration

4.2.1 Tagged Z position

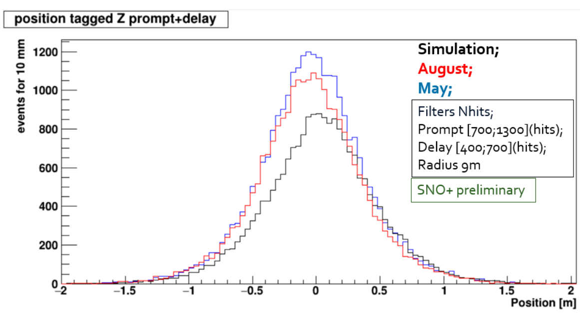

Figure 11. Tagged prompt and delay events in Am-Be calibration source Z axis position for both data and MC simulation.

As showed by the plots in Figure 11 the Z position of the events has similar variance and mean value in May and August, while the simulation has a higher variance and a shift in the mean value of about 8cm. Likely, the shift in position, has to do with how the source was "placed" in the simulation.

		Mean	Sigma
Simulation	**Delay**	0.03694	0.3810
	Prompt	0.03089	0.4504
May	**Delay**	-0.03528	0.3612
	Prompt	-0.03246	0.4329
August	**Delay**	-0.05388	0.3626
	Prompt	-0.04693	0.4303

Table 4. Table of the fitted Z position for both data and simulation using a normal distribution. Mean values in meters (m).

Table 4 shows what was described previously in better detail: We can see the large shift in the Z mean position from the simulation where we get 7 to 9 cm difference when compared to the data for the delay event and 6 to 8 cm difference for the prompt event.

The larger sigma value of the distribution, certainly represents a deeper issue with the simulation. While in the data the sigmas are similar, in the simulation the sigma has been overestimated by 5% in the delay event and 4% in the prompt event.

4.2.2 Radial position of tagged events

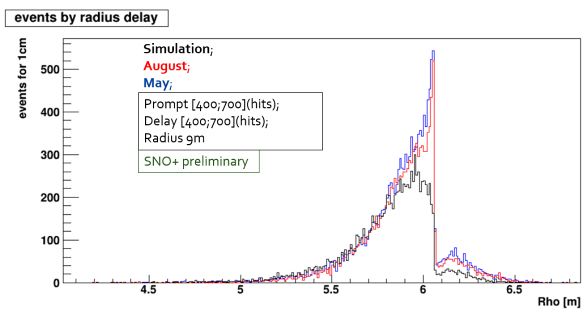

Figure 12. Plot of delay events as a function of ρ ($\rho = \sqrt{x^2 + y^2}$) for both data and simulations.

Figure 12, shows again a discrepancy between simulation and data, The data shows that a higher concentration of delay events happens in the outer layer of the acrylic. When we look to the simulation there isn't any sign of the outer layer concentration that we see in the data, on the contrary, simulation predicts a decrease in the concentration of events inside the acrylic and in the outer layer.

The potential explanation of the different behavior between simulation and data at the acrylic border is a mismodeling of the optical properties of the acrylic itself, therefore creating a difference in the efficiency of detection ultimately generating these increase in concentration of events in the data[2].

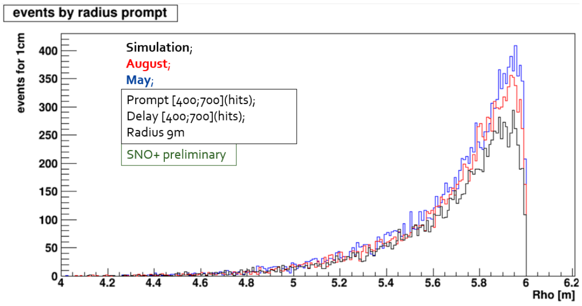

Figure 13. Plot of prompt events as function of ρ for both data and simulations.

Doing the same analysis for the prompt events (see Figure 13) shows a much more similar distribution for the events in data and MC.

5 Conclusion

In this work have shown the comparison between calibration data taken using Am-Be source in two separated campaigns May, right after the completion of the PPO addition, and August 2022. Furthermore, I have compared results with simulations. When looking at the reconstructed energy, calibration shows a large discrepancy, predicting the data up to 10%. A revision of the scintillator and acrylic optical models to better match data at large radii, is therefore advised to have a better prediction for analysis that will use large fiducial volumes.

These values were studied using the Nhits selector due to the bias in the energy selector where, some events, outside the AV were ignored. This was seen as a loss of coincidences in the 10-200μs range. Using the Nhits selector and a large radius, the plot resembles again a half-life capture time of 148 ± 3 μs consistent with the MC.

6 Acknowledgements

I would like to use this space to thank LIP and the team responsible for organizing the internships, as well as a special thank to my supervisor Dr. Valentina Lozza for the opportunity, availability and guidance throughout my internship. Would also like to thank Dr. Sofia Andringa for her help and guidance solving some of the problems found. This was a very enriching experience from which I learned not only physics but also what a research environment is, strengthening my desire to pursue such career.

References

[1] V Lozza and the SNO+ collaboration 2012 J. Phys.: Conf. Ser. 375 042050.

[2] Anderson, M. R., et al. "Measurement of neutron-proton capture in the SNO+ water phase." Physical Review C 102.1 (2020): 014002.

[3] Alexander, Roger L., Daniel Fieno, and C. Hubbard Ford. "Tests of Evaluated Beryllium (n, 2 n) Cross Sections by Analysis of 1.4-eV Flux in Water for an Americium-Beryllium Source Enclosed in Beryllium Spheres." Nuclear Science and Engineering 44.1 (1971): 95-102.

[4] Inácio, A. S. "Data Analysis of the Water and Scintillator Phases of SNO+: from Solar Neutrino Measurements to Double Beta Decay Sensitivity Studies." (2022).

[5] Chen, Jinxiang, et al. "Measurement of partial neutron spectrum of an Am-Be (α, n) source". No. INDC (CPR)–004/L. International Atomic Energy Agency, 1985.

[6] Marsh, J. W., D. J. Thomas, and M. Burke. "High resolution measurements of neutron energy spectra from AmBe and AmB neutron sources." Nuclear Instruments and Methods in Physics Research Section A: Accelerators, Spectrometers, Detectors and Associated Equipment 366.2-3 (1995): 340-348.

[7] Erik Odeblad & Giuseppe Nati (1955) Detection of Beryllium by Means of the Be9 (α, nγ)C12 Reaction, Acta Radiologica, 43:3, 249-255, DOI: 10.3109/00016925509172768

[8]Atomic Data and Nuclear Data Tables 80, 1– 34 (2002) doi:10.1006/adnd.2001.0870

[9]Moeller, E., & Sjoestrand, N.G. (1963). Measurement of the Slowing-Down and Thermalization Time of Neutrons in Water (AE–125). Sweden

[10] High precision neutron inelastic cross sections on 16O Boromiza Marian, et al. EPJ Web Conf. 239 01013 (2020) DOI: 10.1051/epjconf/202023901013